TASK QUARTERLY 10 No 4, 391–400

THE EFFECT OF SELECTED MATERIAL PARAMETERS ON THE STRESS AND STRAIN STATES IN THE PROCESS OF CUTTING A SHEET PLATE WITH CIRCULAR CUTTERS

ŁUKASZ BOHDAL AND LEON KUKIEŁKA

Department of Operating Machinery, Koszalin University of Technology, Raclawicka 15–17, 75-620 Koszalin, Poland
BohdalL@interia.pl, leon@tu.koszalin.pl

(Received 21 August 2006; revised manuscript received 10 September 2006)

Abstract: The influence of the type of material on deformations and stresses of sheet metal in the process of cutting with numerical tools is presented. The Cowper-Symonds model is used to describe the properties of cut sheet-plate and the influence of two parameters C and P on the state of stresses and strains in steel cutting element. Numerical results were obtained by the finite element method (FEM) making use of the ANSYS LS-DYNA ver. 9.0 program, based on the explicit time method.

Keywords: stresses, strains, Cowper-Symonds model, FEM, explicit time method

1. Introduction

Cutting is the process of forming objects which consists in separating one part of material from another [1]. Such separation is accompanied by large plastic strains, which lead to disturbances in the material's coherence. In order to cut a material at the required cross-section a concentration of strains has to be produced in this place capable of overcoming the material's coherence. The simplest method for obtaining such concentration consists in exerting the required pressure on the surface of a sheet plate by means of two edges. Cutting with circular tools is a cutting method leading to cracking due to tensile stress. Cracking of the material occurs in the cross-section weakened by the previously produced strain.

The aim of the present work has been to investigate the effect of the C and P parameters of Cowper-Symonds material model on the state of sheet-metal deformation in the course of the cutting process.

2. The method

The problem was approached using the central-difference method, also referred-to as the explicit-integration method. It includes a few special techniques for direct integration of dynamic equations of motion.

The equation describing an object's motion at a typical time step in updated Lagrangean description assumes the following well-known form [2]:

$$\begin{aligned}&[\boldsymbol{M}]\{\Delta\ddot{\boldsymbol{r}}\}+[\boldsymbol{C}_T(\cdot)]\{\Delta\dot{\boldsymbol{r}}\}+([\boldsymbol{K}_T(\cdot)]+[\Delta\boldsymbol{K}_T(\cdot)])\{\Delta\boldsymbol{r}\}\\&=\{\Delta\boldsymbol{R}_T(\cdot)\}+\{\Delta\boldsymbol{F}(\cdot)\}+\{\boldsymbol{F}_T(\cdot)\},\end{aligned}\tag{1}$$

where:

$[\boldsymbol{M}]$ – global system-mass matrix at time t,
$[\boldsymbol{C}_T]$ – global system-damping matrix at time t,
$[\boldsymbol{K}_T]$ – global stiffness-increment matrix at time t,
$[\Delta\boldsymbol{K}_T]$ – global object stiffness matrix at the step,
$\{\boldsymbol{F}_T\}$ – global object intrinsic load vector at time t,
$\{\Delta\boldsymbol{F}\}$ – object intrinsic load increment vector,
$\{\Delta\boldsymbol{R}_T\}$ – global object external load increment vector,
$\{\Delta\boldsymbol{r}\}$ – object site displacement increment vector,
$\{\Delta\dot{\boldsymbol{r}}\}$ – object site velocity increment vector,
$\{\Delta\ddot{\boldsymbol{r}}\}$ – object site acceleration increment vector.

Equation (1) is solved with respect to time step by step and is not rearranged before this operation. Usually, system displacement, velocities and accelerations are assumed to be known at time $\tau=t_0$ and respectively equal $\{\boldsymbol{r}_0\},\{\dot{\boldsymbol{r}}_0\},\{\ddot{\boldsymbol{r}}_0\}$, the whole interval is divided into parts Δt in length and each step is used for searching the solution to Equation (1). The balance points of systems affected by external, inertial and acceleration forces could be searched for each moment. The end of each moment of time is simultaneously taken to be the beginning of the next moment [2]. However, the equation is not solvable due to the number of unknowns exceeding the number of equations. With n equations of motion at our disposal, $3n$ of $\{\dot{\boldsymbol{r}}\}$ and $\{\ddot{\boldsymbol{r}}\}$ unknowns are searched for. An approximation by the central-difference method has been applied to express $\{\dot{\boldsymbol{r}}\}$ and $\{\ddot{\boldsymbol{r}}\}$ vectors using the dislocation vectors at moments $t-\Delta t$, t, $t+\Delta t$. The proposed method, which can produce an approximate result only, consists in presenting velocity and acceleration by means of displacements according to the following formulas [3]:

$$\{\dot{\boldsymbol{r}}^t\}=\frac{1}{2\Delta t}(\{\boldsymbol{r}^{t+\Delta t}\}-\{\boldsymbol{r}^{t-\Delta t}\}),\tag{2}$$

$$\{\ddot{\boldsymbol{r}}^t\}=\frac{1}{\Delta t^2}(\{\boldsymbol{r}^{t+\Delta t}\}-2\{\boldsymbol{r}^t\}+\{\boldsymbol{r}^{t-\Delta t}\}).\tag{3}$$

The central-difference method for discretization of the second order in time Equation (1) does not require reversing the stiffness matrix $[\boldsymbol{K}]$, which is an advantage, especially when the both mass and damping matrixes are diagonal. However, its fundamental disadvantage is a lack of unconditional algorithm stability, which requires the selection of the step length after time Δt so that it is smaller than the critical time, Δt_{kr}, depending on the system's properties. ANSYS LS-DYNA posesses an option for the automatic length selection in each step, which makes it more user-friendly.

3. Data for numerical analysis

Computer simulations were carried out using the ANSYS LS-DYNA code in the 9.0 version [3, 4]. The cutting element 42×1mm in dimension fixed in the die block has been subjected to analysis Figure 1.

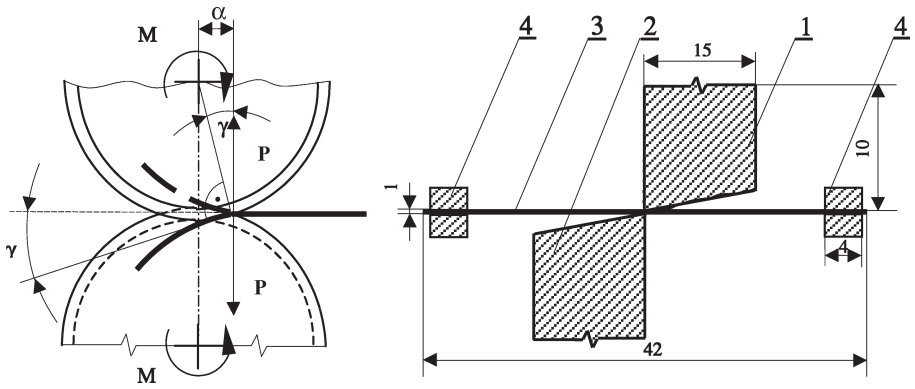

Figure 1. View of test stand: 1, 2 – rotational tools, 3 – cut metal sheet, 4 – plate-gripping tongs

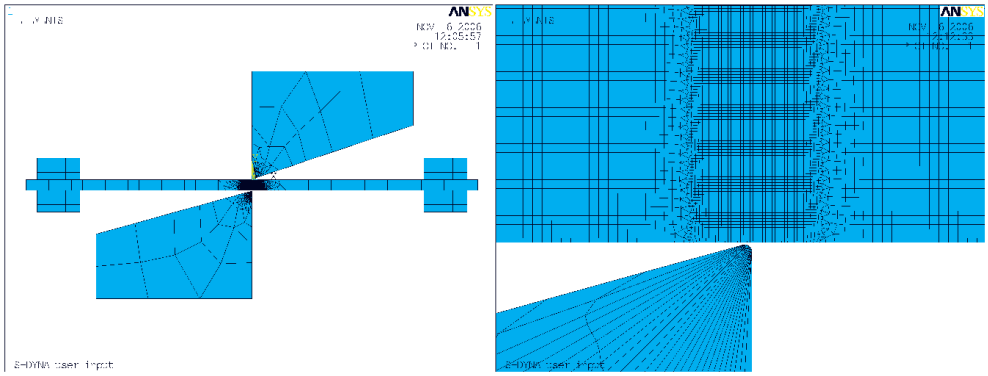

Figure 2. Discrete model of the object

The object was discretizated into finite elements method, selecting an element, which can be thickened in the contact zone (Figure 2).

Undeformable cutting edges were put at a displacement in the material's depth of along the y axis of $u_y = 0.7\,\text{mm}$. The simulation took $t = 0.00001\,\text{s}$. The distance between the tools is $a = 0.01\,\text{mm}$. The maximum value of the plastic strain intensity, the loss of material coherence occours amounted to $\varphi_i^{(\text{dop})} = 1.5$. The sheet plate's density was $\rho = 7800\,\text{kg/m}^3$, the Young modulus – $E = 210\,\text{GPa}$, Poisson's ratio – $\nu = 0.27$, initial static yield point – $R_e = 310\,\text{MPa}$, the modulus of strain hardening – $E_T = 763\,\text{MPa}$, and the strain hardening coefficient – $\beta = 0$. The constant coefficients of static and kinetic friction were respectively assumed to be $\mu_s = 0.08$ and $\mu_d = 0.009$. The die block and cutting tools were assumed to be non-deformable bodies of $E \to \infty$. These values were assumed as constants for each simulation.

4. Material model issues

The Cowper-Symonds elastic/visco-plastic material model was applied in our computer simulations. The Huber-Mises-Hencky yield criterion and the associated law of material flow were utilized in the model. The Cowper-Symonds model allows for linear-isotropic ($\beta = 1$), kinematic ($\beta = 0$, assumed in simulations) or mixed

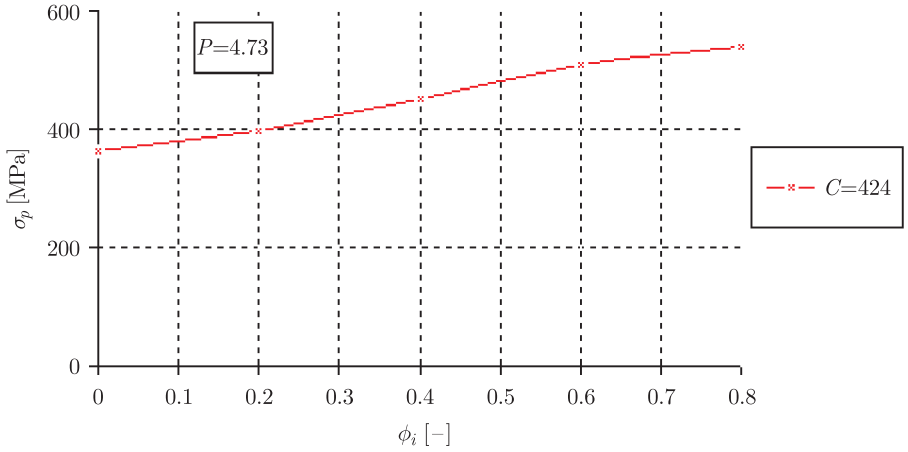

Figure 3. Influence of parameters C [s^{-1}] and P on yield stress for carbon steel ZstE180BH

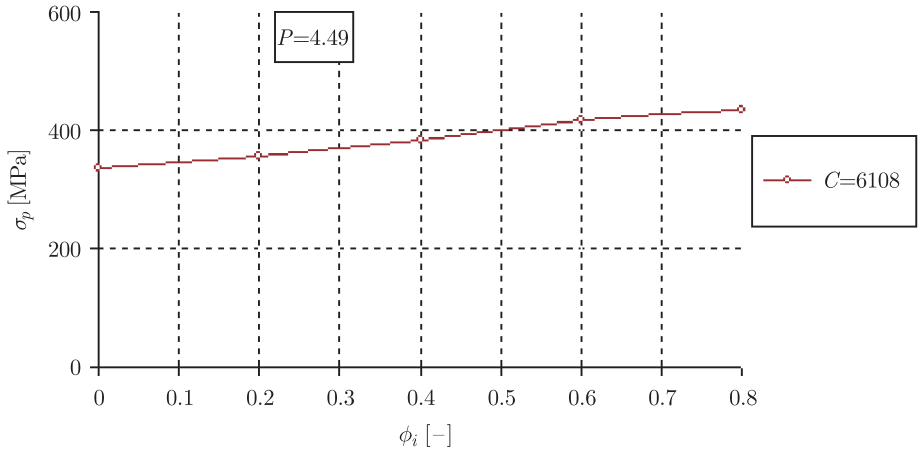

Figure 4. Influence of parameters C [s^{-1}] and P on yield stress for austenitic steel X2CrNiN18

$(0<\beta<1)$ plastic strain hardening and the effect of intensity of plastic strain velocity, in accordance with a power relation [5]:

$$\sigma_p = [1+(\dot{\varphi}_i^{(p)}/C)]^m (R_e + \beta E_p \varphi_i^{(p)}), \tag{4}$$

where

β – the parameter of plastic strain hardening,
R_e – initial, static yield point, [MPa],
$\dot{\varphi}_i^{(p)}$ – the intensity of plastic strain velocity, [s^{-1}],
C – the material parameter defining the effect of intensity of plastic strain velocity, [s^{-1}],
$m = 1/P$ – a material constant defining the material's sensitivity to plastic strain velocity,
$\varphi_i^{(p)}$ – plastic strain intensity,
$E_p = \frac{E_T E}{E - E_T}$ – the material parameter depending on the modulus of plastic strain hardening, $E_T = \partial\sigma_p/\partial\varphi_i^{(p)}$, and the Young modulus, E.

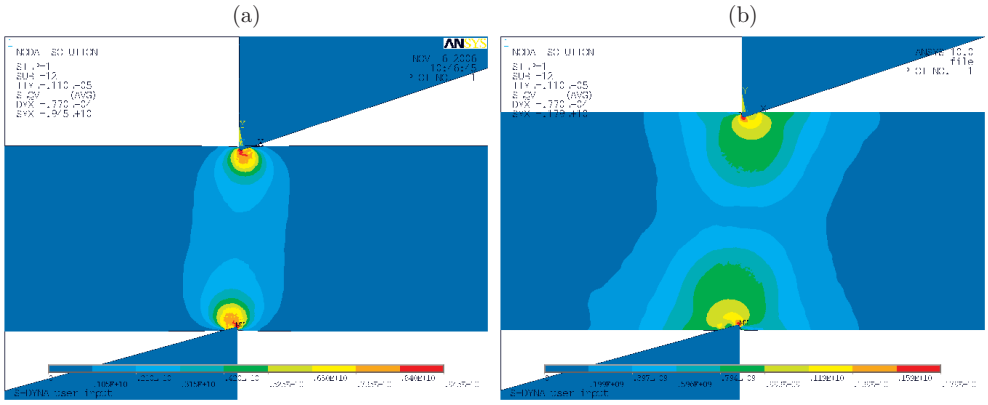

Figure 5. The elastic-plastic phase of the cutting process for (a) $C = 0.1\text{s}^{-1}$, $P = 5$ and (b) $C = 6500\text{s}^{-1}$, $P = 5$

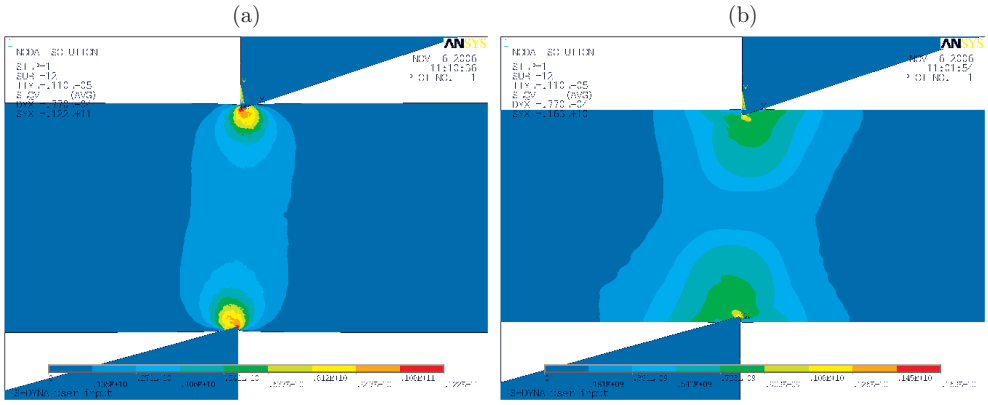

Figure 6. The elastic-plastic phase of the cutting process for (a) $C = 40\text{s}^{-1}$, $P = 3$ and (b) $C = 40\text{s}^{-1}$, $P = 30$

Computer simulations were carried out for the parameter values of $C = 0.1$, 5, 40, 100, 400, 6500s^{-1} and $P = 3$, 5, 30, 80, 500. For example carbon steel ZstE180BH's parameters are $C = 424\text{s}^{-1}$, $P = 4.73$, austenitic steel X2CrNiN18's parameters are $C = 6108\text{s}^{-1}$, $P = 4.49$. Sample results of four simulations are given in Figures 3 and 4.

5. Analytical findings

Sample results of numerical calculations of strain intensity distribution at various stages of the cutting process and various materials ($C = 0.1$, 40 and 6500s^{-1}, $P = 3$, 5, 30) are shown in Figures 5–12.

A plasticised zone in the elastic-plastic phase of strains (Figures 5–6) occurs only at the highest concentration of stresses, that is in direct contact with the cutting edges [6]. As the pressure increases, the cutting edges penetrate the material forming a contact surface sufficiently large to resist the increasing pressure. As the value of parameter C increases, the zone of strain intensity expands to cover a larger part of a plate cross-section. At the same time, the area of critical stresses decreases. The

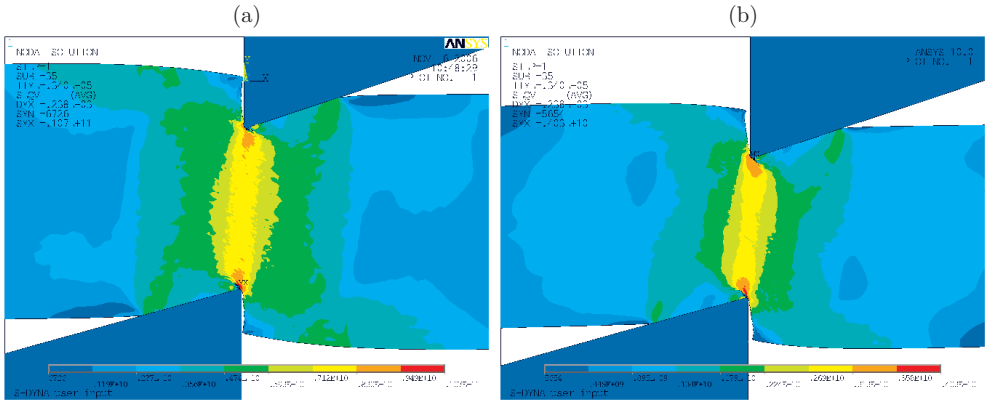

Figure 7. The plastic flow phase of the cutting process for (a) $C = 0.1\text{s}^{-1}$, $P = 5$ and (b) $C = 40\text{s}^{-1}$, $P = 5$

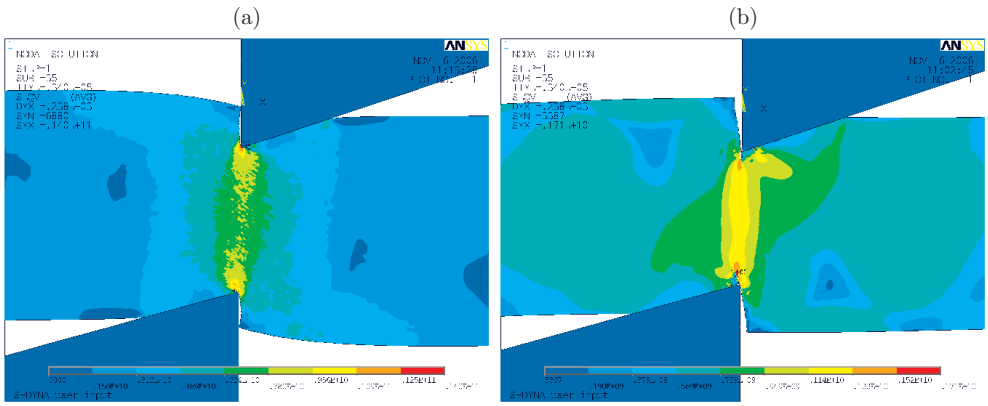

Figure 8. The plastic flow phase of the cutting process for (a) $C = 40\text{s}^{-1}$, $P = 3$ and (b) $C = 40\text{s}^{-1}$, $P = 30$

value of stresses decreases as the value of parameter C increases. A decrease in critical strains was also observed with increasing parameter P.

The plastic flow phase (Figures 7–8) is marked by intensive plastic flow of the material in the surroundings of the cutting surface. It begins at the moment of joining the plastic zones and spreading the plasticized zone over the whole thickness of the plate, which is conductive to conditions enabling the formation of very large plastic strains. A characteristic burr formation can observe under the cutting edges, due to excessive squeezing of the material. An increase in the C and P parameters brings about changes in material strains. The material of $C = 40\text{s}^{-1}$ and $P = 5$ is more brittle than in the other cases. Critical stresses in this material equal 4030MPa.

As the material is subjected to strain hardening, there is also an increase in shear stresses occurring on the cutting surface. At this moment they can reach the critical value at which the material's coherence is disturbed and a cracking phase is initiated (Figures 9–11). The first cracks appear in the areas subjected to the largest strains, *i.e.* close to the cutting edges. The cracks diverge from the edges and meet forming a common cracking surface. Its contour depends on the clearance between the cutting edges: when it is minimal (the smallest one applied in simulations), it

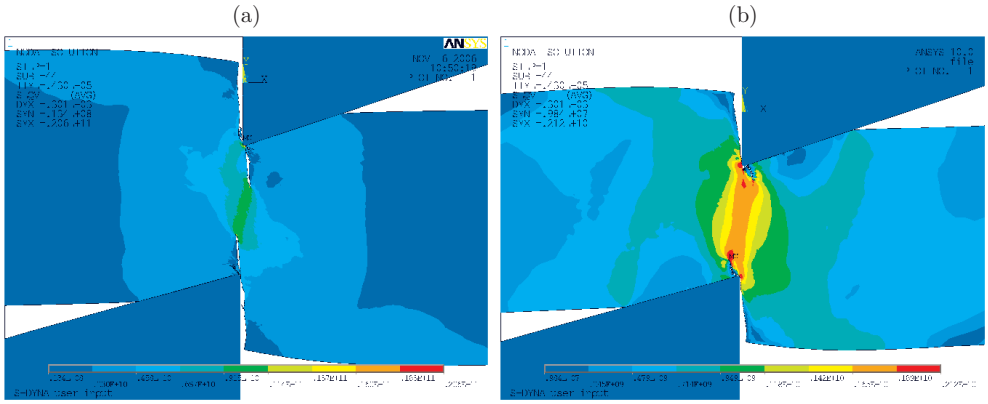

Figure 9. The cracking phase for (a) $C = 0.1\text{s}^{-1}$, $P = 5$ and (b) $C = 6500\text{s}^{-1}$, $P = 5$

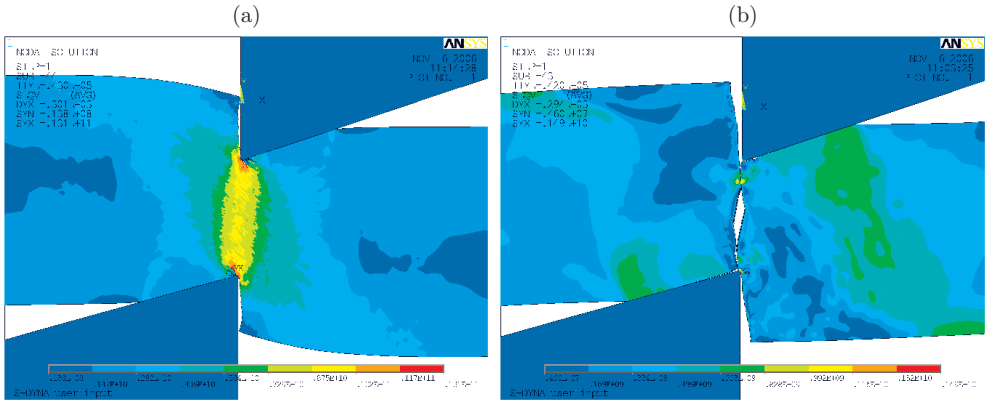

Figure 10. The cracking phase for (a) $C = 40\text{s}^{-1}$, $P = 3$ and (b) $C = 40\text{s}^{-1}$, $P = 30$

is straight; when the clearance is greater, the crack is S-shaped. The application of such small clearance is aimed at obtaining a perpendicular cutting surface and fine smoothness of cutting. If the clearance is too small, the cracking of material is delayed, the phase of plastic strains increases and a smooth cutting surfaced is thus obtained.

Due to increased parameter C the material's cracking is delayed until a further stage of the process. The material of parameter $C = 0.1\text{s}^{-1}$ was subjected to cracking while the phase of separation of the part from the plate was in progress, but the cracking in the material with $C = 6500\text{s}^{-1}$ was just initiated. The first cracks which appeared then were joined and separated the material.

Parameter C has considerable influence on the cracks' shape: its increase has contributed to an increase in burrs on the material's edges (Figure 11). An increase in parameter P accelerates the material cracking process (Figure 10b).

While the $C = 40\text{s}^{-1}$, $P = 30$ material was subjected to total cracking, the material with the $C = 40\text{s}^{-1}$, $P = 3$ characteristics remained in the plastic flow phase slowly transformed into the cracking phase (Figure 11b). Cracking occurred at the final stage of cutting. There also appeared very large critical stresses, which were reduced to 9090 MPa after total cutting.

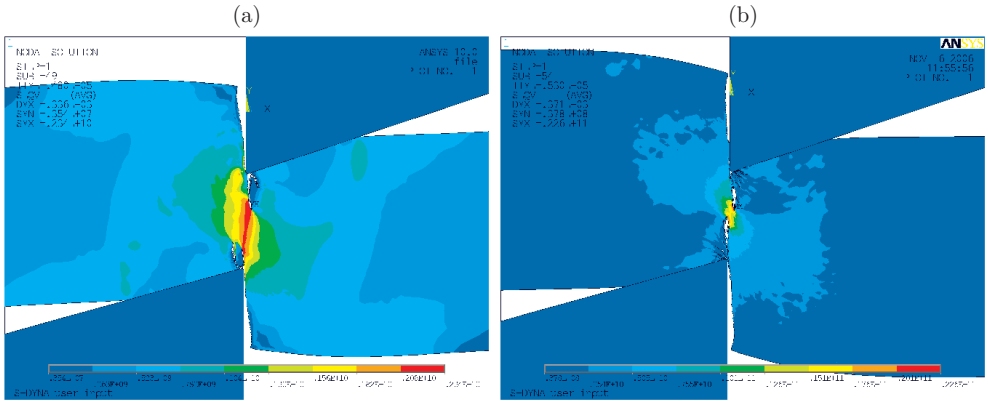

Figure 11. The cracking phase for (a) $C = 6500\,\mathrm{s}^{-1}$, $P = 5$ and (b) $C = 40\,\mathrm{s}^{-1}$, $P = 3$

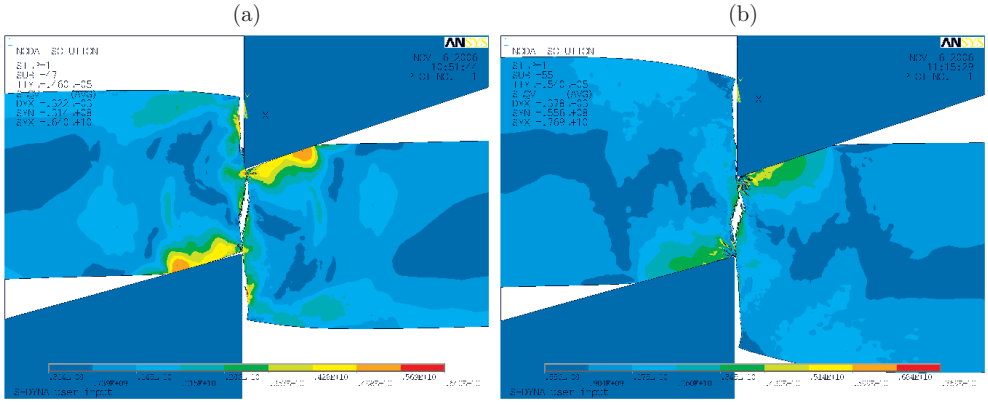

Figure 12. The moment of separating the object from the plate for (a) $C = 0.1\,\mathrm{s}^{-1}$, $P = 5$ and (b) $C = 40\,\mathrm{s}^{-1}$, $P = 3$

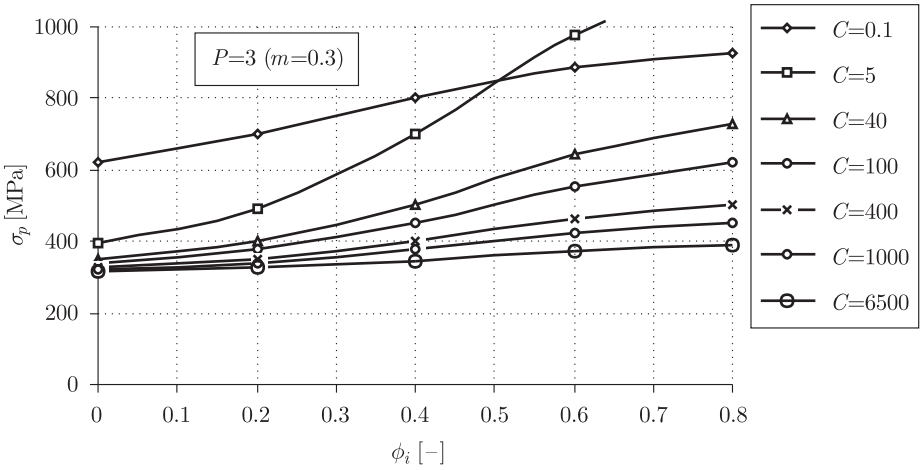

Figure 13. Influence of parameters C [s^{-1}] and P on yield stress for $P = 3$

Diagrams 13–15 illustrate the influence of parameters C and P on yield stress for various values of parameter P.

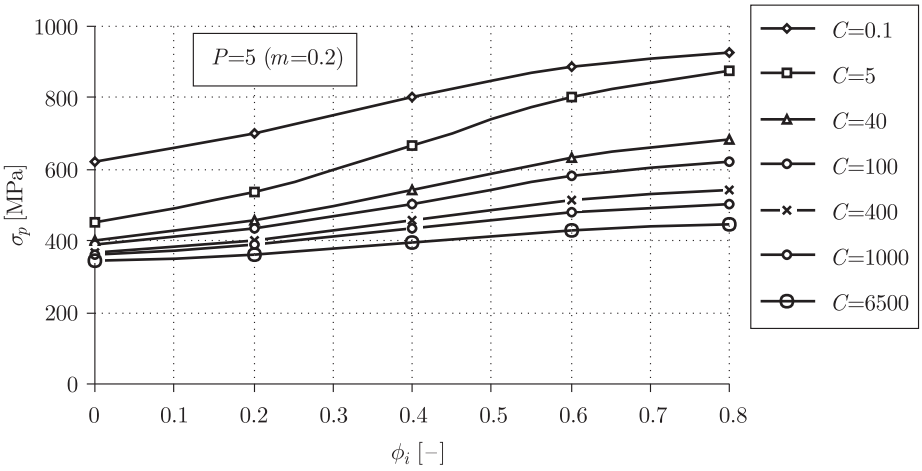

Figure 14. Influence of parameters C [s^{-1}] and P on yield stress for $P = 5$

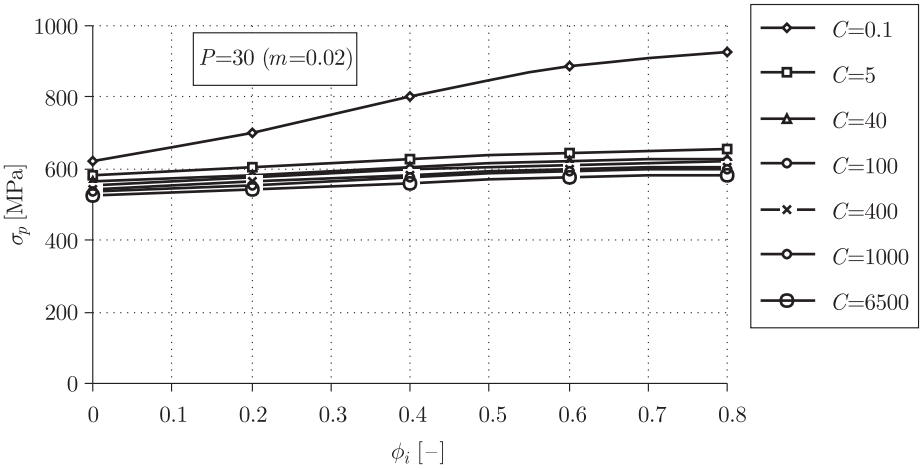

Figure 15. Influence of parameters C [s^{-1}] and P on yield stress for $P = 30$

6. Conclusions

The process of sheet-plate cutting can be construed as a nonlinear boundary-elementary issue. It includes geometric and physical nonlinearity, as well as nonlinear boundary conditions in the contact zone. Although an analytic solution of this problem is unobtainable, it is solvable by the numerical method using the developed application, which allows the process analysis to be applied at any time instant depending on the set parameters of the assumed material model.

The present work describes the effects of parameters C and P of the Cowper-Symonds material model on the state of sheet-plate deformation in the course of cutting. The obtained results have shown that the occurring stresses and strains are significantly differentiated with change parameters C and P. With an increase in parameter C, the range of stress intensification increases covering the larger part of the plate's thickness. However, the range of critical stresses decreases. The value of stresses decreases as the value of parameter C increases. An increase in parameter C

brings about cracking of the material at a further stage of the process. This parameter also exerts great influence on the shape of sheet-plate cracks. In some examples, the shapes of cross-section surfaces have differed significantly, not only in terms of roughness but also the number and size of burrs. An increase in the value of parameter P brings about a decrease in critical stresses and affects the sheet-plate's cracking, simultaneously reducing the material plastic flow phase.

References

[1] Erbel S, Kuczyński K and Marciniak Z 1981 *Plastic Processing*, PWN, Warsaw (in Polish)
[2] Kleiber M 1982 *Finite Element Method in Nonlinear Continuum Mechanics*, PWN, Warsaw-Poznan (in Polish)
[3] Kukiełka L, Patyk R and Wojtalik M 2004 *Numerical analysis states of deformations and stresses in WW object in embossing regular unevenness process*, *Zeszyty Naukowe Wydziału Mechanicznego*, Koszalin, **34** 243 (in Polish)
[4] Huryn S, Kukiełka L and Patyk R 2004 *Analysis of plastic flow of material under stiff wedge effecting*, *VII Słupskie Forum Motoryzacji*, Słupsk, pp. 173–180 (in Polish)
[5] *ANSYS LS-DYNA User's Guide*
[6] Bohdal Ł 2005 *Numerical Analysis of Cutting with Disk Shears*, MSc Thesis, Koszalin University of Technology (in Polish)